

# On the Validation of New Evaluations for the CIELO Project

---

A. Trkov, R. Capote, V.G. Pronyaev

International Atomic Energy Agency, Vienna, Austria

April 2016

## Background

The Working Party on Evaluation Cooperation of the OECD set up a subgroup WPEC-SG40 (alias CIELO) to focus on the evaluated nuclear data of the major nuclides in reactor technology, namely  $^1\text{H}$ ,  $^{16}\text{O}$ ,  $^{56}\text{Fe}$ ,  $^{235}\text{U}$ ,  $^{238}\text{U}$  and  $^{239}\text{Pu}$ . Different research groups in various parts of the world are working on improved evaluated nuclear data and their uncertainties for these nuclides; the ultimate test of improvement is the performance of the data in simulating integral experiments.

An IAEA Coordinated Research Project (CRP) was devoted to the study of prompt fission neutron spectra of actinides. New PFNS evaluations have been provided for uranium and plutonium isotopes in the whole energy range [1]. Additionally, in the on-going IAEA Neutron Standard project it is planned to include  $^{235}\text{U}$  PFNS induced by thermal neutrons as a reference neutron field, and a new fit of Thermal Neutron Constants was done

New sets of Lane consistent Coupled-Channel Dispersive Optical Model Parameters for the actinides have been produced by Capote et al.. This was the starting point for the EMPIRE calculations for  $^{235}\text{U}$  and  $^{238}\text{U}$  to produce cross section data above the resonance range using optical model for fission to describe the resonance behaviour of neutron induced fission cross sections.

Using the information from the above projects and in collaboration with NNDC-BNL at Brookhaven, USA, ORNL at Oak Ridge, USA and IRSN, France, new evaluations for  $^{238}\text{U}$ ,  $^{235}\text{U}$  and the iron isotopes were produced. The evaluated data file for  $^{239}\text{Pu}$  was assembled at LANL, Los Alamos, USA. The oxygen evaluation adopted in the present analysis was produced G. Hale, LANL. The thermal scattering law data for hydrogen in light water were taken from CAB, Bariloche, Argentina.

Detailed description of individual evaluations is in preparation in separate reports. A brief general description of the files is given in the next section.

## File description

The evaluated data files considered in the present analysis are available from the IAEA CIELO web page <https://www-nds.iaea.org/CIELO/> and include the following:

$^{239}\text{Pu}$  The file labelled “239Pu\_ENDF\_LANL\_23c” was obtained from LANL and was processed locally at the IAEA to generate the ACE file for MCNP.

- <sup>238</sup>U The file label is “u238ib46rjFs” and contains:
- <sup>235</sup>U The file label is “u235ib06ao17g6cnu5cf2” and contains
- <sup>56</sup>Fe The file label is “fe56ib15k” and is the result of a complex file assembly based on
- Empire calculation at high energies,
  - Total cross section from JEFF-3.2 in the range 0.85-6.0 MeV,
  - Inelastic cross section in the range 0.86-3.5 MeV based on a combination of measured Dupont and Negret data,
  - JENDL-4.0 resonance parameters (adopted from JEF-2.2 spanning energy range up to 0.85 MeV) with a correction for the resonance energy at 7.667 keV,
  - Angular distributions from JENDL-4.0 up to 0.85 MeV
  - Angular distributions from JEFF-3.2 in the range 0.85-3.5 MeV because they agree with the Kinney data in EXFOR
  - Empire calculation for all other quantities and energies.
- (Gforge version 219).
- <sup>54</sup>Fe The file label is “fe54cielo” and contains BNL evaluation based on a new Empire calculation and resonance parameters from the Atlas (Gforge version 222).
- <sup>57</sup>Fe The file label is “fe57cielo” and contains BNL evaluation based on a new Empire calculation and resonance parameters from the Atlas (Gforge version 234).
- <sup>58</sup>Fe The file label is “fe58cielo” and contains BNL evaluation based on a new Empire calculation and resonance parameters from JEFF-3.2 (Gforge file version 224).
- <sup>16</sup>O The file label is “O16\_haleadx” and contains the evaluation by G. Hale up to 6 MeV. To obtain a full file the cross sections at higher energies were merged with the data from the ENDF/B-VII.1 library. The thermal scattering cross section was reduced, as recommended by C. Lubitz.
- <sup>1</sup>H Thermal scattering law data with file label “h1tsl cab2” were downloaded from the CAB web site [http://www.cab.cnea.gov.ar/nyr/tsl\\_eng.html](http://www.cab.cnea.gov.ar/nyr/tsl_eng.html) which also provides the data in ACE format.

The combined library including all of the above and ENDF/B-VII.1 for the other nuclides is labelled “CIELO20160406”. All calculations presented herein with this label correspond to the data listed above.

## Library Validation

### *Bare assemblies*

The first test was to check criticality prediction of bare assemblies, focusing on <sup>235</sup>U. Several benchmarks can be found in the ICSBEP Handbook, several of them were analysed by Bess et al. and reported at the ND2013 Conference [Bess2013]. Most of them are reproduced in Figure 1. For comparison, the results with the JENDL-4.0 library are also shown. From Figure 1 it is seen that

CIELO20160406 reactivity prediction is systematically higher by a very small amount, in any case smaller than the scattering between different benchmark cases. This implies that bare assemblies are not as “clean” and well-defined as we would like to believe and that the assigned uncertainties are probably underestimated.

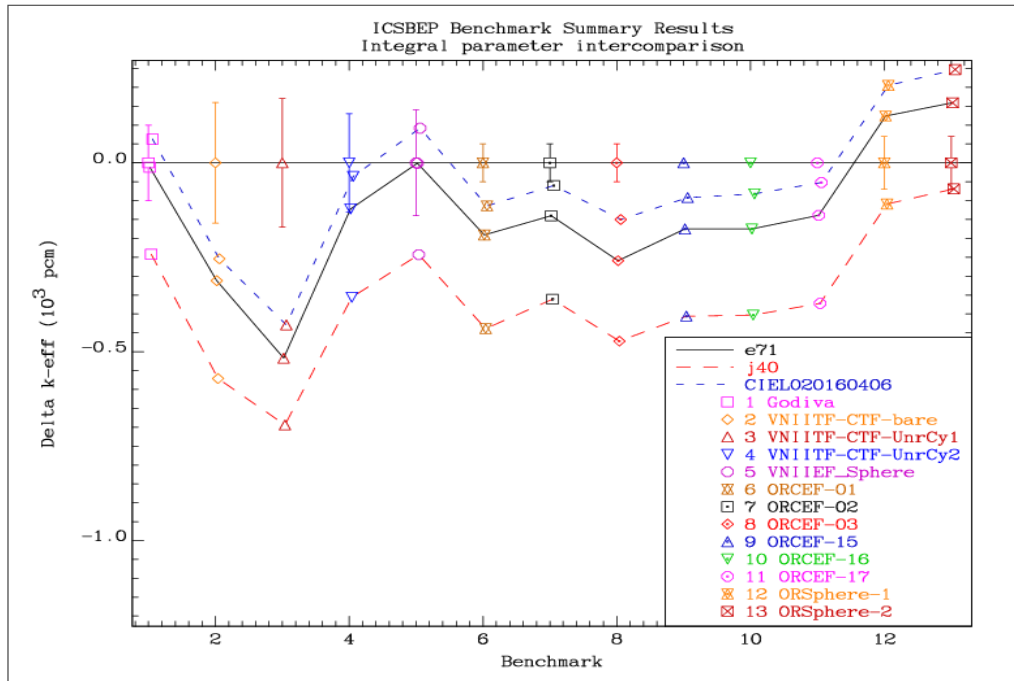


Figure 1: Criticality prediction of bare <sup>235</sup>U assemblies.

### Highly-enriched <sup>235</sup>U solutions

In the paper by A. Kahler [e71\_benchmarking] the importance of reactivity trends as a function of the above-thermal-leakage-fraction (ATLF) was discussed. A similar suite of highly-enriched solution benchmarks (HST) was analysed, but excluding the HEU-SOL-THERM-050 series, because of their large scatter. The results are shown in Figure 2.

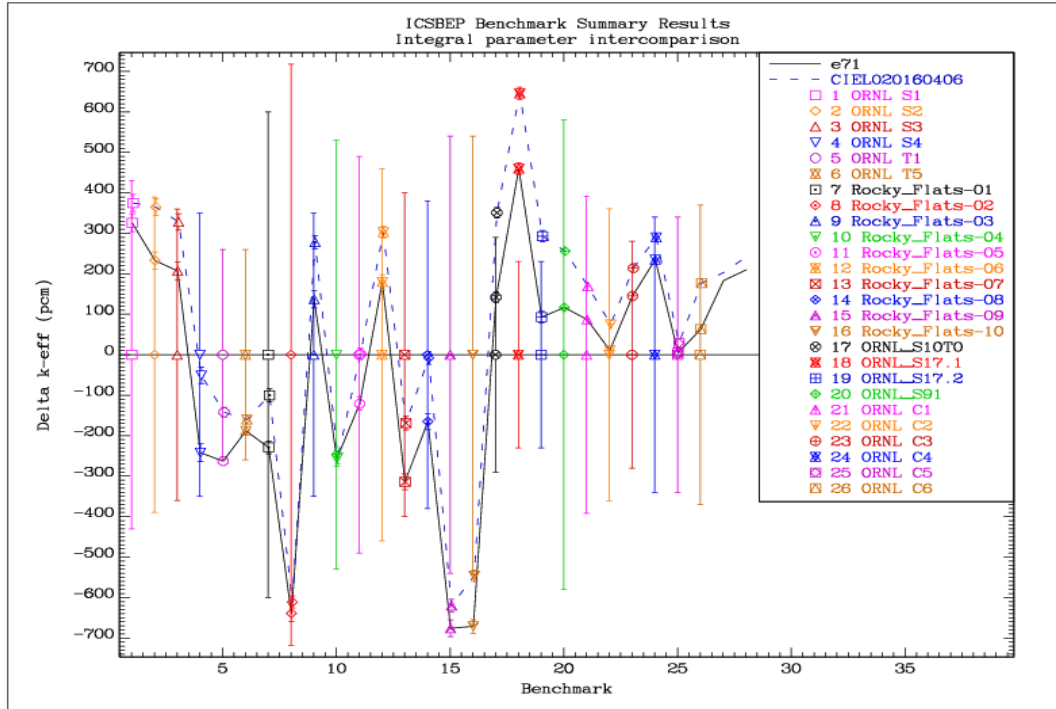


Figure 2: Criticality prediction of highly-enriched solution benchmarks.

The reactivity difference compared to benchmark reference values as a function of ATLF for a short list of representative HST benchmarks is shown in Figure 3. The results are practically all within the experimental uncertainties. Neither the ENDF/B-VII.1 nor the CIELO20160406 results show any excessive gradient. When the full set of benchmarks is analysed, the ENDF/B-VII.1 data are in excellent agreement with the benchmark values (on average), while CIELO results show an offset of about 70 pcm with a slightly positive gradient of 270 pcm/unit\_ATLF. These results differ slightly from those published in [e71\_benchmarking], namely an offset of 70 pcm and a gradient of -100 pcm/unit\_ATLF because the HST050 series benchmarks were omitted in the present analysis and the fitted functional is the difference of the multiplication factor (C-E), while in the reference uses the ratio (C/E). The results confirm that the CIELO20160406 evaluations introduces a minimal positive trend with respect to ATLF.

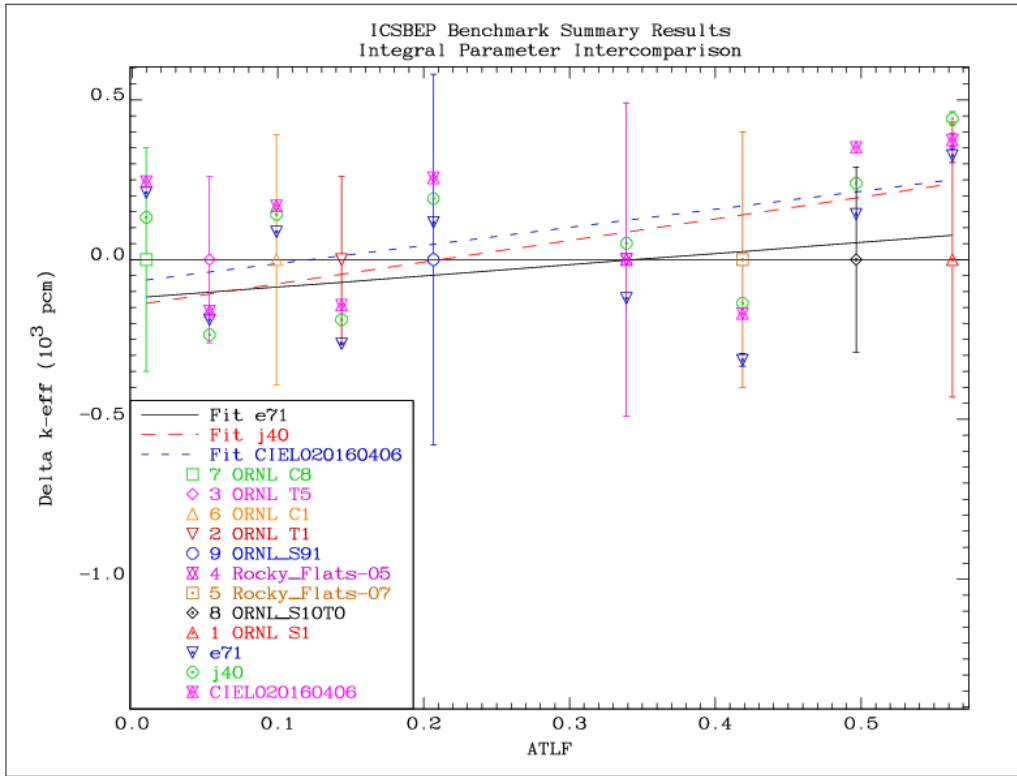


Figure 3: Criticality of representative highly-enriched solution benchmarks as a function of the above-thermal leakage fraction.

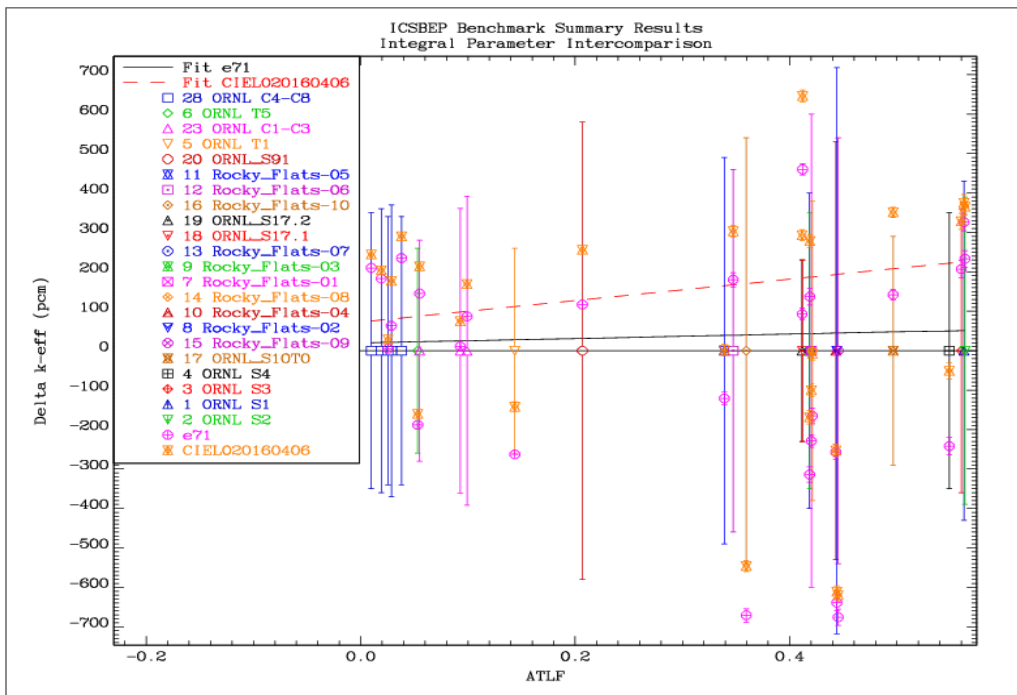


Figure 3a: Criticality of a full set of highly-enriched solution benchmarks as a function of the above-thermal leakage fraction.

## General performance for uranium-fuelled systems

The new evaluated data files were tested on a number of fast and intermediate systems. Compared to ENDF/B-VII.1 several improvements are observed, as seen from Figure 4. The amplitude of differences for the well-known benchmarks Godiva, Flattop-U8 and Big Ten is greatly reduced. The Jemima series is almost within the uncertainty band, although it must be said that the uncertainties are most likely underestimated. Slightly worse results are obtained for Pajarito and the UH3 benchmarks with a thick  $^{238}\text{U}$  reflector. Overall, the “Chi-squared per degree of freedom” figure of merit is reduced from 6.12 to 0.86 for the benchmarks in Figure 4.

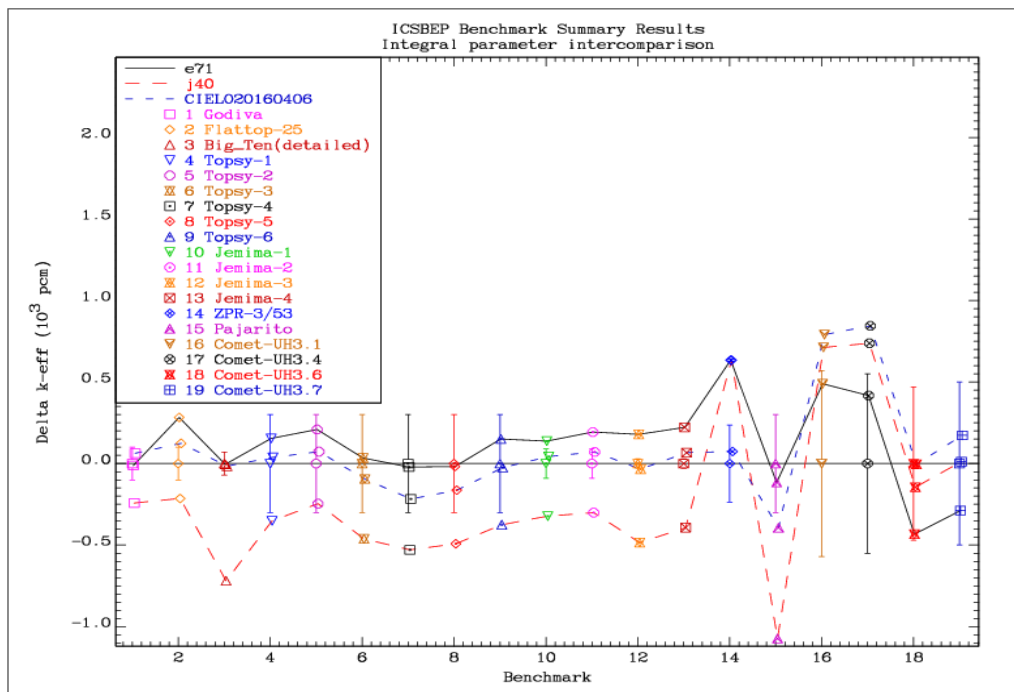


Figure 4: Criticality prediction for uranium-fuelled fast and intermediate assemblies.

## Assemblies with a $^{238}\text{U}$ reflector

In several benchmark series a clear trend is observed as the  $^{238}\text{U}$  reflector thickness increases. For example, the uranium-reflected Topsy series of benchmarks (HEU-MET-FAST-003) with reflector thickness varying from 2.54 cm to 28 cm shows a gradient of about 35 pcm per cm of reflector (see Figure 5). The gradient in another Topsy series (HEU-MET-FAST-032) is practically the same, although the range of reflector thickness variations is smaller, as shown in Figure 6.

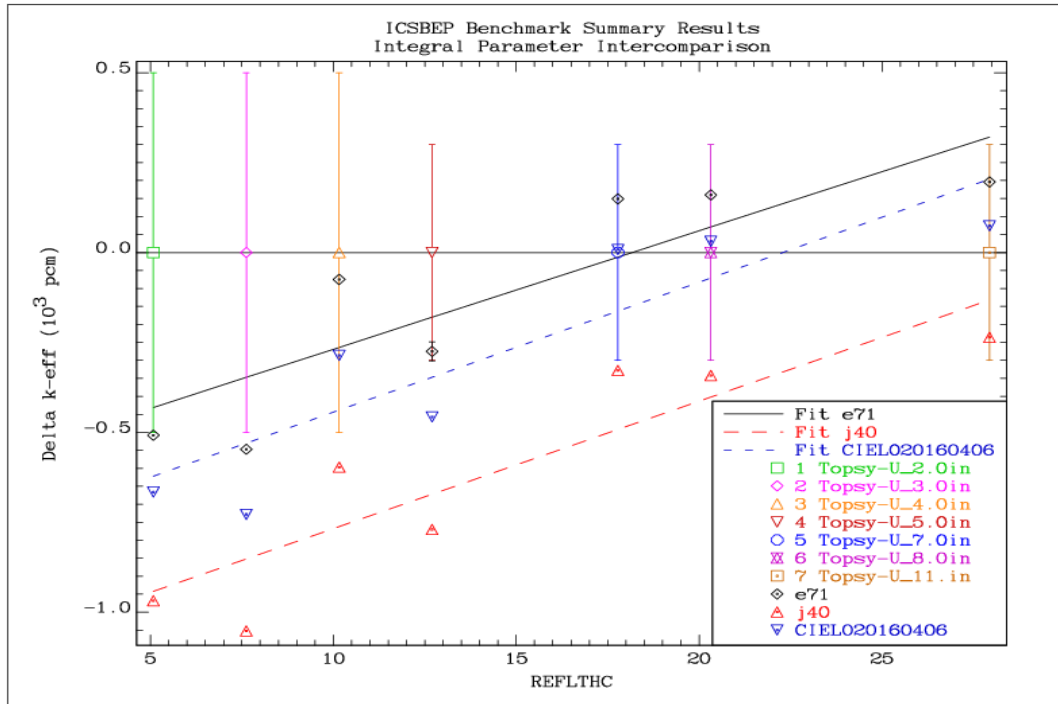


Figure 5: Reactivity difference trend as a function of <sup>238</sup>U reflector thickness [cm] for the Topsy series of benchmarks (HEU-MET-FAST-003).

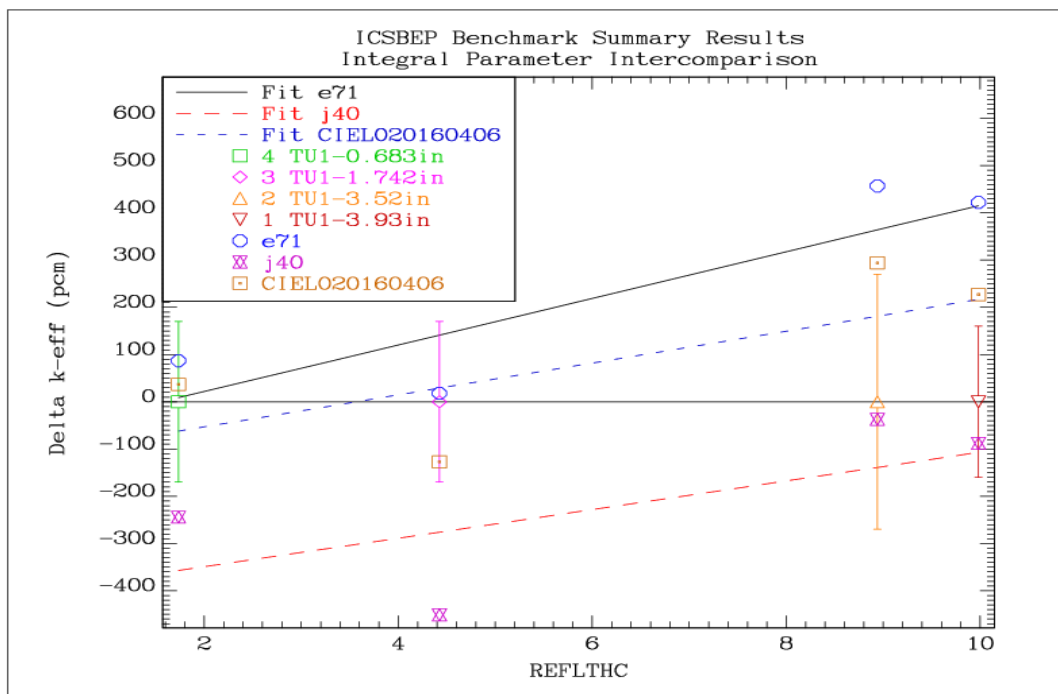


Figure 6: Reactivity difference trend as a function of <sup>238</sup>U reflector thickness [cm] for the Topsy series of benchmarks (HEU-MET-FAST-032).

The following symptoms can be identified:

- Reactor lattices containing  $^{238}\text{U}$  perform well.
- To a first approximation, only fast neutrons can penetrate deep into the  $^{238}\text{U}$  reflector.
- Conversely, only fast neutrons can return back into the core to affect reactivity.

We may conclude that the reactivity is affected by  $^{238}\text{U}$  fission. In principle, the effect could also be due to elastic angular distributions, but it would show up even with thinner reflectors, so we rule-out this option.

The fission cross section is pretty much constrained by the standards and we cannot make large changes to it. We could change  $\nu$ -bar, but the effect is too small, if changes to  $\nu$ -bar are to remain reasonable. We need an effect that will not change the reactivity of reactor systems due to  $^{238}\text{U}$ , except when  $^{238}\text{U}$  appears in the reflector.

The hypothesis is that neutron emission from fission is anisotropic. This would not affect fission in the core, because the flux there is (almost) isotropic, compared to a reflector, where it is strongly outward biased.

Experimental data show that fission fragments emission is anisotropic, with a preferred direction at about 90 degrees. Although the fragments are much heavier than neutrons, they carry much more energy, so their speed relative to an average neutron is smaller by less than a factor of two. Therefore, even when neutron emission from fragments is isotropic in the CM system, they can be strongly anisotropic in the lab system, if the fission fragment distribution is anisotropic (as it is, according to measured data).

The hypothesis thus has some substance, but testing it in practice proves to be difficult. The experts of Monte Carlo codes MCNP, MVP, TART and TRIPOLI were consulted, but it seems that none of the codes is capable of explicitly treating anisotropic distribution of neutrons from fission (MF4/MT18 or MF6/MT18).

Go Chiba from JAEA kindly provided some results of deterministic calculations for two cases of the HEU-MET-FAST-003 benchmark (HMF003 for short) using 175-group library based on JENDL-4.0 data. The results are summarised in Table 1.

Table 1: Impact on k-eff of the HE-MET-FAST-003 benchmark due to Fission Neutron Anisotropy in the reflector (JENDL-4.0 175-group calculation, Go Chiba, private communication 8-April-2016).

Refl.[cm]	Measured	JENDL-4.0	JAEA	P1=0	P1=0.01	P1=0.1
5.08	1.00000	0.99032	0.99065	0.99122	0.99012	0.97997
27.94	1.00000	0.99764	0.99820	0.99952	0.99866	0.99077

The results can be summarized as follows:

- The JENDL-4.0 results for the HMF003 benchmarks are on the low side (in absolute terms), but the deterministic calculations are consistent with those published in JAEA-Data/Code

2011-010 and with our own calculations based on JENDL-4.0 data library. The relative differences from the analysis are valid.

- The sensitivity of k-eff to the P1 coefficient is large and amounts to about -11000 pcm/P1 for the thin reflector and -8700 pcm/P1 for the thickest reflector; the decrease in the latter is reasonable because at nearly 30 cm thickness the reflector savings reach saturation. The sensitivity seems to be practically linear with P1.
- The sensitivity is high, but it seems to be in the opposite direction than expected.

The preferred direction of fission fragments is in the direction orthogonal to the incident neutron. Since the average speed of fission fragments is comparable to the speed of the neutrons, it is reasonable that in the lab system the preferred direction of emitted neutrons would also be peaked at about 90 degrees. This implies a negative P2 coefficient. Sensitivity to the P2 coefficient would be required in addition to P1.

The overall performance of uranium-reflected systems is shown in Figure 7. Generally, the predicted reactivity with CIELO20160406 data is somewhat lower than with ENDF/B-VII.1 data, being in fair agreement with the measured values, except for the Topsy assemblies: the first set has a negative bias with a thin reflector layer, while the second set is high with a thick reflector. Both show a strong trend with reflector thickness, as seen from Figures 5 and 6. The same could also be said for the Comet UH3-1 and -4 assemblies in Figure 4, compared to cases 6 and 7, which only have a thin reflector.

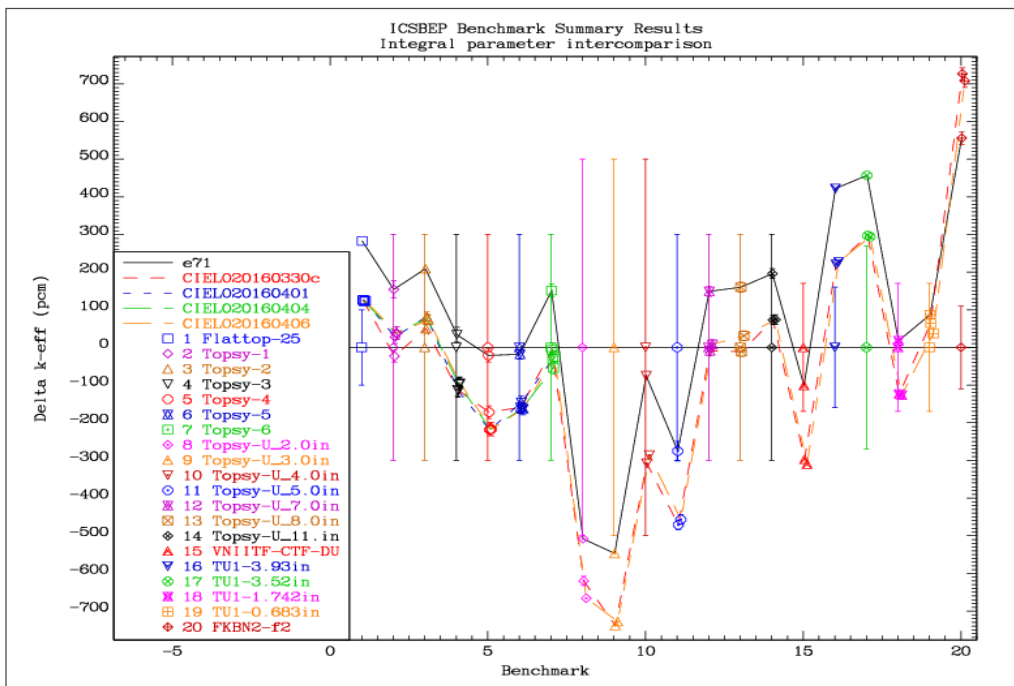


Figure 7: Criticality prediction for uranium-reflected systems.

## Thermal lattices

The reactivity of thermal lattices is predicted by CIELO20160406 data reasonably well, although there is a tendency to underpredict reactivity in cases with a low *energy of the average lethargy causing fission* (EALF). This underprediction is more pronounced than with ENDF/B-VII.1 data, as seen on Figure 7a. Cases 2 to 15 are shown. Case 1 has a very high ATLF; it corresponds to the configuration with a regular lattice of fuel rods without water holes or poison rod inserts and is predicted well. On the plot the individual cases are joined by lines (black =ENDF/B-VII.1, red=CIELO20160406). The straight lines across the plot correspond to a linear fit for each of the two libraries.

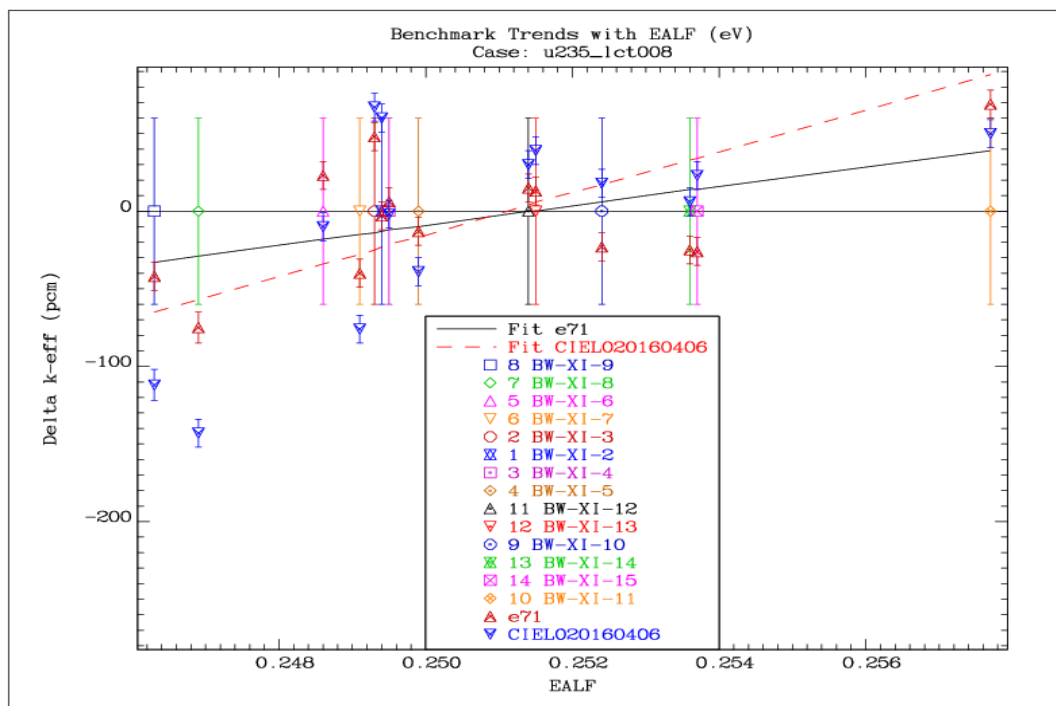


Figure 7a: Criticality prediction of thermal lattices. The plotted uncertainties in measured data are only the uncertainties in the criticality determination.

## Low-enriched solutions

A series of low-enriched nitrate solution STACY benchmarks was performed in Japan, and a few additional ones with fluoride solutions at Oak Ridge. Very good agreement is achieved with ENDF/B-VII.1 as well as with the CIELO20160406 library, as shown on Figure 7b.

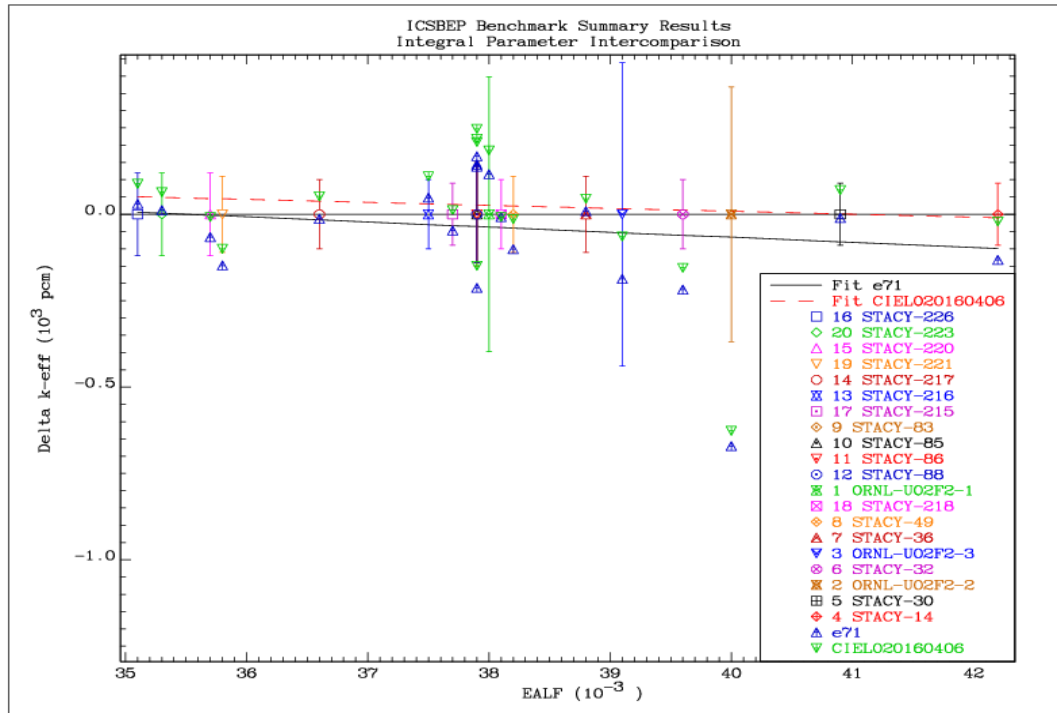


Figure 7b: Criticality prediction of low-enriched solution benchmarks.

### Validation of evaluated nuclear data for the iron isotopes

Iron is a very common structural material, but unfortunately also very difficult to evaluate. A lot of measurements exist for the natural element, as well as for the major isotopic constituent  $^{56}\text{Fe}$  with abundance of 91.75 %. There are several strong scattering resonances in  $^{56}\text{Fe}$ , with very deep interference minima, where the cross section is nearly zero. In these energy intervals the cross sections of the minor isotopes, as well as the alloying constituents (e.g. in stainless steel) dominate. For this reason the evaluation of  $^{56}\text{Fe}$  nuclear data cannot be separated from the evaluations of the minor isotopes and alloying materials.

The results for several benchmarks that are sensitive to iron cross sections are shown in Figure 8. The reactivity of plutonium systems is lower than that using ENDF/B-VII.1 data and is outside the uncertainty band. Assemblies ZPR-6/7, ZPR-9/31 and ZPPR-2 are also predicted worse, but ZPR-9/34 and particularly ZPR-6/10 show significant improvement.

It is also worth noting that switching back to Fe evaluations of ENDF/B-VII.1 is not an option. Due to changes in  $^{238}\text{U}$  and  $^{235}\text{U}$ , particularly the lowering of capture in  $^{235}\text{U}$  would greatly increase the reactivity of assemblies like ZPR-9/34 and ZPR-6/10. Many benchmarks (including the latter two) are highly sensitive to the capture cross section below 25 keV. In this respect the present evaluations represent an ad hoc tuning of the data. The resonance parameters are essentially those of Froehner prepared for JEF-2.2. There is a need to obtain reliable measurements of the (capture) cross sections of  $^{56}\text{Fe}$  and the minor isotopes (as well as alloying elements like Cr) in the energy range 10-25 keV. A thorough re-evaluation of the resonance parameters is needed, if significant progress is to be achieved.

Above the resonance range the cross sections seem to be in order, except that the (n,2n) cross section of  $^{56}\text{Fe}$  needs to be checked.

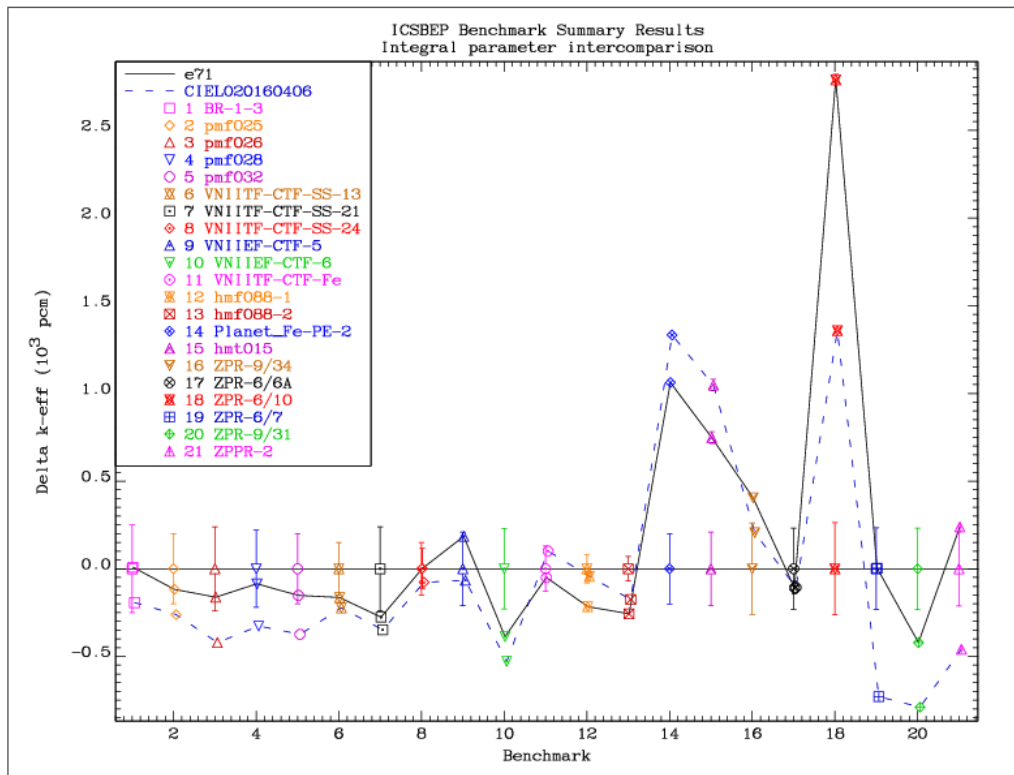


Figure 8: Criticality prediction of systems containing iron.

### Improvements since November 2015

A number of benchmarks were identified for which the new evaluations performed worse than ENDF/B-VII.1. Since then, significant progress was made, as shown on Figure 9. The older version of the library is labelled "o16fe56u5u8". The problem of thermal lattices of the BW-XI series is almost eliminated. The first four Comet-UH3 assemblies have a thick reflector of depleted uranium. They could be subject to the problem discussed above regarding the  $^{238}\text{U}$  reflected systems.

Note the single point on the plot for Case 8 referring to ZPR-9/34; the point corresponds to a calculation including all iron files from ENDF/B-VII.1 and demonstrates that we cannot switch back to it. The calculated reactivity is high due to a decrease in the capture in  $^{235}\text{U}$ , which is solidly supported by new measurements (Jandel, n\_TOF).

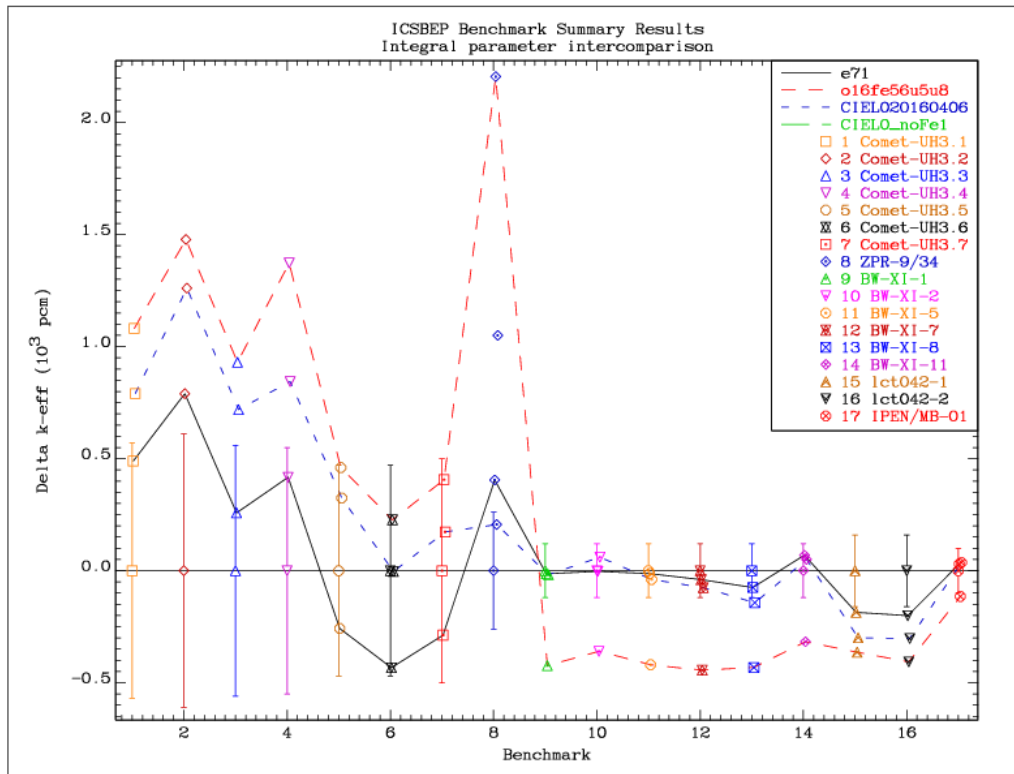


Figure 9: Improvement in performance of the new evaluations since November 2015.

## Conclusions

The results need to be analysed carefully because they depend not only on individual nuclide evaluations but also on the compensating effects between them. In general, there is marked improvement in the predicted reactivity of uranium-fuelled systems. Less attention was devoted to the plutonium and  $^{233}\text{U}$  systems. Specifically,

- Highly-enriched bare assemblies have trends very similar to ENDF/B-VII.1, with a slightly positive offset, but the scattering of the results is unchanged and exceeds experimental uncertainties. Differences in data sensitivities are small, therefore it is unlikely that by tuning the data the spread in the results would be decreased. The uncertainties in the measured data or in the benchmark specifications are probably larger than estimated.
- Highly-enriched uranium solutions are in very good agreement with the measured data, comparable to ENDF/B-VII.1 No significant trend as a function of the above thermal leakage fraction is observed.
- Benchmarking on a broader range of fast and intermediate spectrum systems shows a significantly reduced spread of the calculated reactivities compared to the benchmark reference values.
- There seems to be some trend of increased differences from benchmark reactivity values with increasing thickness of  $^{238}\text{U}$  reflector, which is similar to the results with the ENDF/B-VII.1 data. The root-cause of this trend has not been identified yet. One possibility are the angular distributions of elastic scattering of  $^{238}\text{U}$  in the resonance range, but the anisotropy of neutrons emitted from fission in  $^{238}\text{U}$  are also considered. Unfortunately, none

of the Monte Carlo codes commonly used for benchmarking can take anisotropic fission neutron distributions into account.

- Plotting the reactivity difference between the calculated and benchmark values as a function of the energy of the average lethargy causing fission (EALF) a trend is observed that is slightly bigger than with the ENDF/B-VII.1 data. We hope that an improvement will be achieved with updated capture and fission data of  $^{235}\text{U}$  in the energy range above 10 eV.
- Benchmarks involving iron are particularly problematic because of strong compensating effects. Essentially, we cannot claim improvement with the use of the new evaluations for the iron isotopes. Recent changes in the  $^{235}\text{U}$  and  $^{238}\text{U}$  evaluations, which are solidly justified, exclude the use of the old ENDF/B-VII.1 evaluations. More work on the iron evaluations is needed. Particularly, an update to the resonance parameters of  $^{56}\text{Fe}$ , simultaneously with the minor isotopes is badly needed. New measurements of the capture cross sections in the 10-25 keV region (i.e. the “window” below the 25 keV resonance) are required to pin-down the cross sections in this energy range. Re-evaluation of the resonance parameters of the chromium isotopes in the same energy interval is also needed, since this isotope is a major constituent of stainless steel.

One can claim that significant progress was made since November 2015. Reactivity prediction of thermal lattices has been improved. It is not perfect, but we expect some improvement with the improved capture and fission data of  $^{235}\text{U}$  above 10 eV. The UH3 assemblies with a thick reflector of depleted uranium also show some improvement, but the predicted reactivities are still well above the benchmark values and outside the uncertainty band. These benchmarks are also expected to improve with updated  $^{235}\text{U}$  data above 10 eV. The improvement in the predicted reactivities of ZPR-9/34 and ZPR-6/10 assemblies is due to a somewhat ad hoc tuning of capture of  $^{56}\text{Fe}$  below 25 keV, but at least the extremely high sensitivity to this particular energy range has been identified so that more effort can be put into the evaluation of the resonance parameters in this energy range.

In short, good progress was made, but we are not ready yet to “declare victory”.

## References

- [1] R. Capote et al, “Prompt Fission Neutron Spectra of Actinides”, Nucl. Data Sheets 131 (2016) 1.
- [2] J.D. Bess, J.B. Briggs, M.A. Marshall: “What if Lady Godiva Was Wrong?”, International Conference on Nuclear Data for Science and Technology (ND 2013).
- [3] A.C. Kahler et al.: ENDF/B-VII.1 Neutron Cross Section Data Testing with Critical Assembly Benchmarks and Reactor Experiments, Nuclear Data Sheets 112, 12 (2011).

## APPENDIX

### ICSBEP labels, short names and common names of ICSBEP benchmarks

Bare U-235 assemblies		
HEU-MET-FAST-001	hmf001	Godiva
HEU-MET-FAST-008	hmf008	VNIIEF-CTF-bare
HEU-MET-FAST-015	hmf015	VNIIEF-CTF-UnrCy1 500 pcm low with ENDF/B-VII.1
HEU-MET-FAST-065	hmf065	VNIIEF-CTF-UnrCy2
HEU-MET-FAST-018	hmf018	VNIIEF_Sphere
HEU-MET-FAST-051	hmf051-01	ORCEF-01
HEU-MET-FAST-051	hmf051-02	ORCEF-02
HEU-MET-FAST-051	hmf051-03	ORCEF-03
HEU-MET-FAST-051	hmf051-15	ORCEF-15
HEU-MET-FAST-051	hmf051-16	ORCEF-16
HEU-MET-FAST-051	hmf051-17	ORCEF-17
HEU-MET-FAST-100	hmf100-1	ORSphere-1
HEU-MET-FAST-100	hmf100-2	ORSphere-2
Highly-enriched uranium systems		
HEU-MET-FAST-001	hmf001	Godiva
HEU-MET-FAST-028	hmf028	Flattop-25
IEU-MET-FAST-007	imf007d	Big_Ten (detailed)
HEU-MET-FAST-002	hmf002-1	Topsy-1
HEU-MET-FAST-002	hmf002-2	Topsy-2
HEU-MET-FAST-002	hmf002-3	Topsy-3
HEU-MET-FAST-002	hmf002-4	Topsy-4
HEU-MET-FAST-002	hmf002-5	Topsy-5
HEU-MET-FAST-002	hmf002-6	Topsy-6
IEU-MET-FAST-001	imf001-1	Jemima-1
IEU-MET-FAST-001	imf001-2	Jemima-2
IEU-MET-FAST-001	imf001-3	Jemima-3
IEU-MET-FAST-001	imf001-4	Jemima-4
MIX-MET-INTER-004	mmi004	ZPR-3/53
IEU-MET-FAST-002	imf002	Pajarito
HEU-COMP-INTER-003	hci003-1	COMET-UH3-1 Refl.D38/D38
HEU-COMP-INTER-003	hci003-4	COMET-UH3-4 Refl.D38/Fe
HEU-COMP-INTER-003	hci003-6	COMET-UH3-6 Refl.none/D38
HEU-COMP-INTER-003	hci003-7	COMET-UH3-7 Refl.none/D38
U-238 reflected systems		
HEU-MET-FAST-028	hmf028	Flattop-25
HEU-MET-FAST-002	hmf002-1	Topsy-1
HEU-MET-FAST-002	hmf002-2	Topsy-2
HEU-MET-FAST-002	hmf002-3	Topsy-3
HEU-MET-FAST-002	hmf002-4	Topsy-4
HEU-MET-FAST-002	hmf002-5	Topsy-5
HEU-MET-FAST-002	hmf002-6	Topsy-6
HEU-MET-FAST-003	hmf003-01	Topsy-U_2.0in
HEU-MET-FAST-003	hmf003-02	Topsy-U_3.0in
HEU-MET-FAST-003	hmf003-03	Topsy-U_4.0in
HEU-MET-FAST-003	hmf003-04	Topsy-U_5.0in
HEU-MET-FAST-003	hmf003-05	Topsy-U_6.0in
HEU-MET-FAST-003	hmf003-06	Topsy-U_8.0in
HEU-MET-FAST-003	hmf003-07	Topsy-U_11.in
HEU-MET-FAST-014	hmf014	VNIIEF-CTF-DU
HEU-MET-FAST-032	hmf032-1	COMET-TU1_3.93in
HEU-MET-FAST-032	hmf032-2	COMET-TU2_3.52in
HEU-MET-FAST-032	hmf032-3	COMET-TU3_1.742in
HEU-MET-FAST-032	hmf032-4	COMET-TU4_0.683in
HEU-MET-FAST-052	hmf052	KFBN2-f2
Highly-enriched solution systems		
HEU-SOL-THERM-009	hst009-1	ORNL_S1
HEU-SOL-THERM-009	hst009-2	ORNL_S2
HEU-SOL-THERM-009	hst009-3	ORNL_S3
HEU-SOL-THERM-009	hst009-4	ORNL_S4
HEU-SOL-THERM-013	hst013-1	ORNL_T1
HEU-SOL-THERM-013	hst013-2	ORNL_T2
HEU-SOL-THERM-013	hst013-3	ORNL_T3
HEU-SOL-THERM-013	hst013-4	ORNL_T4
HEU-SOL-THERM-032	hst032	ORNL_T5
HEU-SOL-THERM-001	hst001-01	R01
HEU-SOL-THERM-001	hst001-02	R02

HEU-SOL-THERM-001	hst001-03	R03
HEU-SOL-THERM-001	hst001-04	R04
HEU-SOL-THERM-001	hst001-05	R05
HEU-SOL-THERM-001	hst001-06	R06
HEU-SOL-THERM-001	hst001-07	R07
HEU-SOL-THERM-001	hst001-08	R08
HEU-SOL-THERM-001	hst001-09	R09
HEU-SOL-THERM-001	hst001-10	R10
HEU-SOL-THERM-010	hst010-1	ORNL_S10T0
HEU-SOL-THERM-011	hst011-1	ORNL_S17.1
HEU-SOL-THERM-011	hst011-2	ORNL_S17.2
HEU-SOL-THERM-012	hst012	ORNL_S91
HEU-SOL-THERM-042	hst042-1	ORNL_C1
HEU-SOL-THERM-042	hst042-2	ORNL_C2
HEU-SOL-THERM-042	hst042-3	ORNL_C3
HEU-SOL-THERM-042	hst042-4	ORNL_C4
HEU-SOL-THERM-042	hst042-5	ORNL_C5
HEU-SOL-THERM-042	hst042-6	ORNL_C6
HEU-SOL-THERM-042	hst042-7	ORNL_C7
HEU-SOL-THERM-042	hst042-8	ORNL_C8

Low-enriched solution benchmarks

LEU-SOL-THERM-002	lst002-1	ORNL-UO2F2-1
LEU-SOL-THERM-002	lst002-2	ORNL-UO2F2-2
LEU-SOL-THERM-002	lst002-3	ORNL-UO2F2-3
LEU-SOL-THERM-007	lst007-14	STACY-14
LEU-SOL-THERM-007	lst007-30	STACY-30
LEU-SOL-THERM-007	lst007-32	STACY-32
LEU-SOL-THERM-007	lst007-36	STACY-36
LEU-SOL-THERM-007	lst007-49	STACY-49
LEU-SOL-THERM-010	lst010-83	STACY-83
LEU-SOL-THERM-010	lst010-85	STACY-85
LEU-SOL-THERM-010	lst010-86	STACY-86
LEU-SOL-THERM-010	lst010-88	STACY-88
LEU-SOL-THERM-020	lst020-216	STACY-216
LEU-SOL-THERM-020	lst020-217	STACY-217
LEU-SOL-THERM-020	lst020-220	STACY-220
LEU-SOL-THERM-020	lst020-226	STACY-226
LEU-SOL-THERM-021	lst021-215	STACY-215
LEU-SOL-THERM-021	lst021-218	STACY-218
LEU-SOL-THERM-021	lst021-221	STACY-221
LEU-SOL-THERM-021	lst021-223	STACY-223

Iron benchmarks

PU-MET-FAST-015	pmf015	BR-1-3
PU-MET-FAST-025	pmf025	pmf025
PU-MET-FAST-026	pmf026	pmf026
PU-MET-FAST-028	pmf028	pmf028
PU-MET-FAST-032	pmf032	pmf032
HEU-MET-FAST-013	hmf013	VNIITF-CTF-SS-13
HEU-MET-FAST-021	hmf021	VNIITF-CTF-SS-21
HEU-MET-FAST-024	hmf024	VNIITF-CTF-SS-24
IEU-MET-FAST-005	imf005	VNIIEF-CTF-5
IEU-MET-FAST-006	imf006	VNIIEF-CTF-6
HEU-MET-FAST-087	hmf087	VNIITF-CTF-Fe
HEU-MET-FAST-088	hmf088-1	hmf088-1
HEU-MET-FAST-088	hmf088-2	hmf088-2
HEU-MET-THERM-013	hmt013-2	Planet_Fe-2
HEU-MET-THERM-015	hmt015	
HEU-MET-INTER-001	hmi001	ZPR-9/34
IEU-COMP-INTER-005	ici005	ZPR-6/6A
PU-MET-INTER-002	pmi002	ZPR-6/10
MIX-COMP-FAST-001	mcf001	ZPR-6/7
MIX-COMP-FAST-005	mcf005-s	ZPR-9/31
MIX-COMP-FAST-006	mcf006-s	ZPPR-2

Big outlier range)